Fuel 116 (2014) 191–200

Contents lists available at ScienceDirect

Fuel

journal homepage: www.elsevier.com/locate/fuel

Application of porous medium approach to simulate UCG process

Mojtaba Seifi, Jalal Abedi *, Zhangxin Chen

Department of Chemical & Petroleum Engineering, University of Calgary, Calgary, Canada

HIGHLIGHTS

- Describing main assumptions in order to adapt the porous medium approach for UCG simulation.
- Developing relationships between basic analyses on coal and required parameters for porous medium simulators.
- Developing a numerical simulation model for pyrolysis process using porous medium approach.
- Simulating self-gasification process in cylindrical coal using hydrocarbon simulators.

ARTICLE INFO

Article history:
Received 14 May 2013
Received in revised form 23 July 2013
Accepted 23 July 2013
Available online 8 August 2013

Keywords:
Pyrolysis
Self-gasification
Modeling
Hydrocarbon simulator
Porous medium

ABSTRACT

Underground coal gasification (UCG) is a promising technique where coal is converted into valuable syngas in underground reactors developed in coal seams. This method is of paramount interest due to its lower cost, the ability to access coal at greater depths, and the utilization of oil and gas technologies and previously drilled wells to reach the coal seams. In this study, the main assumptions of a porous medium approach for the simulation of the UCG process are explained in detail. Moreover, the formula and procedure to obtain the required parameters through hydrocarbon reservoir simulators are presented. The proposed method is evaluated with three case studies. Computer Modelling Group's STARS software is used in this study.

1. Introduction

Underground coal gasification (UCG) is a technique for the utilization of coal reserves, particularly at great depths where mining is not economical. UCG is an in situ process that converts solid fuel to synthetic gas (syngas) in the presence of steam and oxygen. This process has only a modest environmental impact and produces an easily transportable product. The intended uses of this syngas include the production of electrical power and chemicals [1,2].

UCG involves the gasification of coal in the seam by injecting oxidants through an injection well and extracting the syngas through a production well. The configuration of these wells implies different technologies, such as linked vertical wells, steeply dipping seams, linear controlled retracting injection point (CRIP), and parallel CRIP.

Due to the low permeability nature of the coal seams, the injection and production wells are linked by a channel, which can be developed with several proven techniques, such as reverse combustion, hydraulic fracturing, and directional drilling. Coal is then ignited around the injection point, producing a cavity as coal is combusted and gasified. In the area between the internal cavity surface and the original coal, several phenomena take place that control the heat and mass fluxes within the solid porous coal around the cavity. These phenomena include a gas film on the internal surface of the cavity, an ash layer on the cavity surface, pyrolysis, self-gasification, vaporization of the moisture content, and possible water inflow.

As shown in Fig. 1, the cavity itself can be divided into two parts: first, rubble material at the bottom of the cavity around the injection point, which may include ash, dry char and coal spalling and collapsing from the top of the cavity, and overburden materials; and second, void space on the top of the rubble materials, containing a gas mixture. In this void space, the temperature and concentration of the gas mixture may vary over time. As a result, there is a double-diffusive, turbulent-free convection flow that controls the transportation of the gaseous reactants from the bulk of the gas to the surface of the cavity [2–4].

UCG is a complex process; its modeling is crucial in order to understand the details of the process and the effect of different operating parameters on the objective parameters, such as the quality, rate and composition of the produced syngas, and the growth rate and shape of the developed cavity. For decades,

* Corresponding author. Address: 2500 University Dr., NW, Calgary, Alberta T2N 1N4, Canada. Tel.: +1 403 220 5594; fax: +1 403 282 4852.
E-mail address: jabedi@ucalgary.ca (J. Abedi).

0016-2361/$ - see front matter © 2013 Elsevier Ltd. All rights reserved.
http://dx.doi.org/10.1016/j.fuel.2013.07.091

Nomenclature

A_0	frequency factor, variable unit
A_{0i}	frequency factor of evolution of *i*th species, 1/s
C_S^o	initial coal concentration (daf basis), mol/m^3 pore volume
E_a	activation energy, kJ/mol
E_{ai}	activation energy of evolution of *i*th species
k_g	thermal conductivity of gas mixture, J/m-day-K
k_r	thermal conductivity of rock (ash), J/m-day-K
k_s	thermal conductivity of solid fuel (char and coal), J/m-day-K
k_w	thermal conductivity of water, J/m-day-K
m_i	cumulative amount of *i*th volatile matter released by time *t*, g
m_i^*	initial amount of *i*th volatile matter can be released during pyrolysis, g
MW_c	carbon (char) molecular weight, kg/mol
MW_{daf_coal}	dry-ash-free (daf) coal molecular weight, g/mol
MW_i	molecular weight of species *i*, g/mol
R	gas constant, 8.314 J/mol-K
T	temperature, K
x_{ash}	mass percentage of coal ash content
x_{H2O}	mass percentage of coal moisture content

Greek letters

β	heating rate, °C/min
ρ_a^o	initial ash solid density, kg/m^3
ρ_{wat}^o	water density at coal seam initial condition, kg/m^3
ρ_{wc}^o	initial wet coal bulk density, kg/m^3
$\emptyset_f$	fluid porosity
$\emptyset_f^o$	initial fluid porosity
$\emptyset_v$	void porosity of the system
$\emptyset_v^o$	initial void porosity

researchers have been developing models to investigate specific aspects of this process. These models include the channel model, the packed bed model, the coal block model, and the process model.

Channel models assume a cylindrical coal seam with a channel in the middle with either a circular or rectangular cross section. The diameter of the internal channel can be fixed or variable. These models can be used to investigate the composition of the produced gas and the cavity growth rate through heterogeneous reactions. Packed bed models consider coal as a highly permeable dry or wet porous medium. These models are useful in the prediction of the composition of the product gas. In coal block models, wet or dry coal is assumed to have very low permeability in a one-dimensional (1D) semi-infinite domain. One side of this block is exposed to a mixture of gas mimicking the bulk gas mixture within the cavity and is ignited. This allows for the prediction of the rate of pyrolysis, the fire front advancement, and the temperature profile inside the coal ahead of the fire front. Process models are very simplified models used to investigate the effects of specific phenomena, such as water influx, spalling, and flow properties inside the cavity [3-10].

All the current models in the literature are, however, small scale models and need to satisfy certain assumptions on the shape of the cavity, such as cylindrical or rectangular. In these models, the effects of different well configurations, coal seam geology and layering cannot be investigated, and large-scale simulation cannot be performed. Therefore, the application of hydrocarbon reservoir simulators for modeling of the UCG process has been proposed previously by the authors [11].

Since oil and gas reservoirs have a different nature than that of coal seams, the major assumptions for the utilization of these porous medium based simulators for the UCG process are explained in this paper. A procedure and formulas are proposed to obtain the required information for the model from basic elemental and proximate analyses of coal and ash. The assumptions and procedure are evaluated with three case studies. The first case is the qualitative evaluation of the model according to a heavy oil in situ combustion tube test. Case two matches the results of an analytical method for modeling of the pyrolysis process using this proposed method. Finally, case three is the simulation of the self-gasification experiment. The agreement between the results of the proposed simulation model and the analytical and experimental results confirms the validity of this method.

2. Simulation domain structure

The existence of a rock structure in hydrocarbon reservoirs is the major difference between coal seams and hydrocarbon reservoirs, particularly those of heavy oil. In coal seams, there is a large volume of very low porous coal that is composed of moisture,

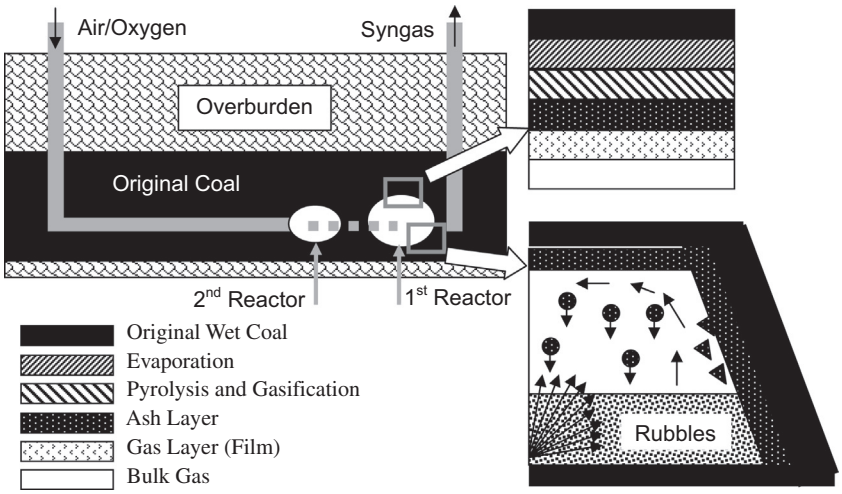

Fig. 1. Schematic of linear CRIP and underground cavities with relevant phenomena.

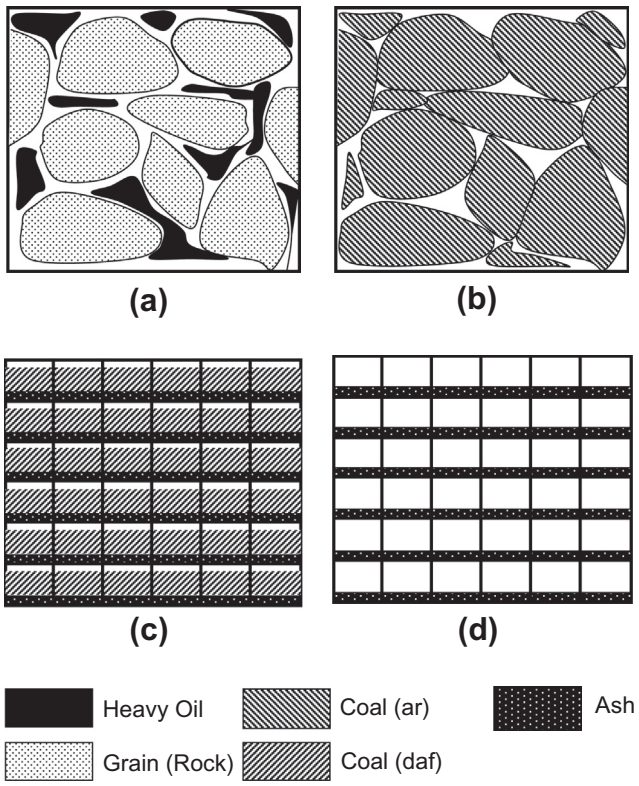

Fig. 2. Schematic of domain structures: (a) heavy oil reservoir, (b) coal seam, and (c) and (d) a coal seam in the simulation model before and after gasification and combustion, respectively.

flammable material, and ash minerals. Since ash remains nearly intact at the end of the UCG process, it can be assumed that ash forms the rock structure of a porous medium simulation model. The moisture content of coal, therefore, resembles the initial water saturation of a hydrocarbon reservoir model; and, the flammable material is similar to the model's solid heavy oil content, which will undergo pyrolysis, gasification and combustion processes. Fig. 2 illustrates this concept.

All the moisture content of coal is separated from the solid phase; hence, the flammable portion of the coal is assumed to be dry coal. With this approach, there is no evaporation phenomenon, which takes place in real field cases. Thus, to offset this deficiency, the evaporation of the water phase is considered in the proposed model. In addition, the pore volume is initially assumed to be filled with the moisture content of coal and gas, i.e., mostly methane (CH_4). Moreover, since ash is separated from the other solid materials to construct the rock network of the model, the solid fuel is considered to be on dry-ash-free (daf) basis.

Another approach is the assumption that the initial pore volume is only filled with gas and that the solid flammable material includes the moisture content of coal as well, i.e., wet coal. In this case, the moisture content must be released by an evaporation reaction in which wet coal is converted into steam and dry coal. The usual evaporation–condensation of water must be included as in the first approach.

3. Seam physical properties

Due to the differences between the natures of coal seams and hydrocarbon porous media, there are several required physical parameters needed for simulation that have rarely been obtained experimentally; therefore, they must be calculated from the coal proximate and ultimate analyses based on the following approach. Some of these important parameters are the coal's molecular weight, the initial void porosity, and the initial concentration of coal in the unit pore volume of the seam, the initial coal solid density, and the initial char density. For simplicity, char is assumed to be a pure carbon, such as graphite, because char is the product of the pyrolysis process and consists of mostly carbon, depending on the rank of coal.

Using material and volume balances, a set of relationships has been developed to relate the results of the coal analysis tests and the required parameters for the simulation model. In this procedure, it is assumed that the ash solid density, the water density at the initial coal seam conditions and the wet coal bulk density are known. The ash density can be obtained from elemental and ash analysis tests. Moreover, it is assumed that the initial pore volume is filled entirely with the coal moisture content. The latter assumption may introduce a very small inaccuracy due to the initial existence of gas, but due to very low initial porosity of the coal seam, it does not have a significant effect on the estimation of the properties. Eqs. (1)–(5) can be used to calculate the above properties.

$$MW_{daf\_coal} = \frac{100MW_C}{x_c} \tag{1}$$

$$\emptyset_V^o = 1 - \frac{x_{ash} \cdot \rho_{wc}^o}{\rho_a^o} \tag{2}$$

$$C_S^o = \frac{1000\rho_{wc}^o(1 - x_{H2O} - x_{ash})}{\emptyset_V^o.MW_{daf\_coal}} \tag{3}$$

$$\emptyset_f^o = \frac{\rho_{wc}^o \cdot x_{H2O}}{\rho_{wat}^o} \tag{4}$$

$$\rho_{daf\_coal}^o = \left(\frac{\emptyset_V^o}{\emptyset_V^o - \emptyset_f^o}\right)\left(\frac{C_S^o \cdot MW_{daf\_coal}}{1000}\right) \tag{5}$$

In cases where partings are dispersed in the coal and cannot be considered as a separate parting layer, the determination of the initial fluid porosity from experiments is necessary. The difference of this fluid porosity and the one calculated from Eq. (4) can then be deducted from the initial void porosity obtained with Eq. (2), which implies the addition of this amount to the rock volume. The initial coal content and coal solid density can then be recalculated with Eqs. (3) and (5).

4. Fluid properties

Generally, the coal pore volume is initially filled with water and gas, which is mostly composed of CH_4. During the simulation process, other gas components, such as carbon oxides, and hydrogen (H_2), are also introduced to the proposed model. Therefore, in addition to the initial properties of water and gas, some physical and thermal properties of other components must be entered into the model.

5. Case studies

5.1. Case 1: combustion tube test

The combustion tube test is an important test in the heavy oil in situ combustion process. The fuel type, the air requirement, the maximum temperature during the combustion process, and the rate of advance of the fire front can be obtained from this experiment. This information can be used either for pilot design or

Table 1
Coal analysis results.

Proximate analysis (ar, wt%)		Ultimate analysis (daf, wt%)	
Moisture	4.72	H	5.56
Ash	9.28	C	73.49
Volatile matter	30.46	N	1.54
Fixed carbon	55.54	S	0.52
		O	18.89
Total	100.00	Total	100.00

large-scale simulation. Due to the similarity of UCG to the heavy oil in situ combustion process, a 1D horizontal model has been developed using the above assumptions, in order to investigate the physical behavior of the model and generate the combustion tube results qualitatively. The domain was discretized into 100 grid blocks sized 5 * 1 * 1 cm. Oxygen (O_2) was injected into the first block, and syngas was produced from the last block. In order to initiate the ignition of coal, the injection block was heated for 1 day, and O_2 was then injected at a rate of 0.3 sm^3/day.

In this model, six gas components (H_2, O_2, CH_4, water (H_2O), carbon dioxide (CO_2), and carbon monoxide (CO) and two solid components (dry-ash-free coal and char) have been considered. The initial pressure and temperature were assumed to be 11.5 MPa and 60 °C, respectively, which are typical values of Alberta's coal seams at great depths. Table 1 summarizes the results of the ultimate and proximate analysis of the coal used for this model. Table 2 shows the applied eight first-order Arrhenius-type reactions in this model. They are the common reactions in a UCG process. The reaction kinetics was obtained from the literature [3,12].

Fig. 3 illustrates the typical temperature and solid concentration profiles. The temperature increased from the injection temperature to the oxidation temperature and then leveled off to the pyrolysis temperature, due to endothermic reactions. At the end, the temperature tended to be the original temperature of the seam. This temperature profile corresponds to the behavior of the heavy oil in situ combustion test. Before the maximum temperature, all the produced char was consumed by heterogeneous reactions; and, the char concentration then increased to the maximum level, where complete pyrolysis occurred. The reduction of the char concentration at a temperature around 500 °C indicates the occurrence of partial pyrolysis. Beyond this point, the coal concentration increased to the initial value.

As shown in Fig. 4, the mole fraction of CO_2 increased to a maximum at the highest temperature, due to the oxidation reaction, and then declined to zero, due to the Boudouard reaction. Carbon dioxide was also produced as a result of the pyrolysis process ahead of the fire front.

The volume-weighted thermal conductivity of the system was calculated according to Eq. (6). The drastic change in the combined

Table 2
Applied reactions in simulation model of Case 1.

Reaction name	Reaction formula	A_0	E_a (kJ/mol)
Carbon oxidation	$C + O_2 \rightarrow CO_2$	1.80E+06	100
Steam gasification	$C + H_2O \rightarrow H_2 + CO$	4.70E+07	156
Buodouard	$C + CO_2 \rightarrow 2CO$	3.20E+10	249
Methanation	$C + 2H_2 \rightarrow CH_4$	1.56E+08	200
Pyrolysis	$daf_{coal} \rightarrow C, CO, CO_2, H_2, CH_4$	1.90E+14	180
Carbon monoxide (CO) Oxidation	$CO + 0.5O_2 \rightarrow CO_2$	9.68E+12	247
Water–gas shift	$CO + H_2O \leftrightarrow CO_2 + H_2$	2.40E+05	12.6
Steam-methane reforming	$CH_4 + H_2O \leftrightarrow CO + 3H_2$	2.70E+07	30

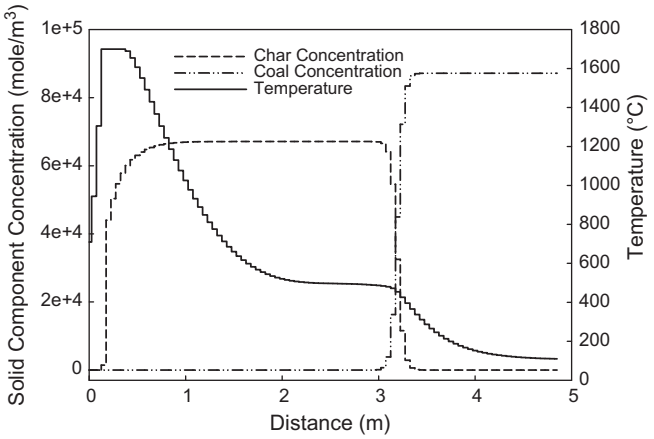

Fig. 3. Temperature and solid component concentration profiles at 2.5 days.

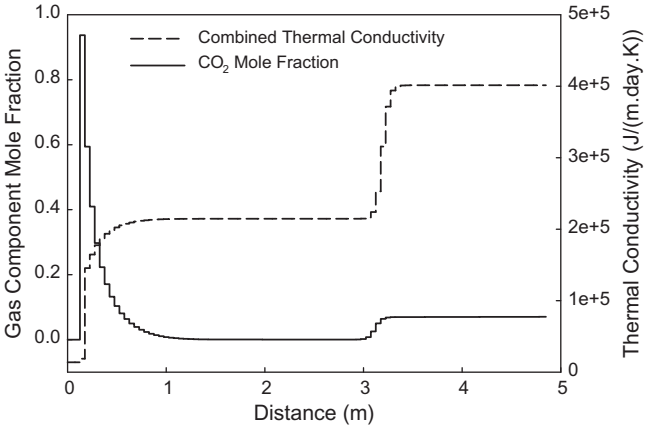

Fig. 4. Carbon dioxide and porous medium thermal conductivity at 2.5 days.

thermal conductivity is an indication of variation in the solid content of the domain. When there was only ash as the solid component, the thermal conductivity began from a very small value, since the medium was filled with gas with lower thermal conductivity. The thermal conductivity increased to an intermediate value, when char also existed in the system. Finally, it reached a maximum value, corresponding to the original seam with the highest solid content.

$$k_{mix} = \emptyset_f \cdot (k_w \cdot S_w + k_g \cdot S_g) + (1 - \emptyset_v) \cdot k_r + (\emptyset_v - \emptyset_f) \cdot k_s \quad (6)$$

The rate of advance of the fire front can be determined from the location of the maximum temperature and the maximum mole fraction of CO_2, as shown in Figs. 5 and 6, as these two parameters have their highest value at the location of the oxidation reaction. For the current configuration, the fire front advancement rate was approximately 15 cm/day.

Fig. 7 shows the coal concentration profiles at various times. The sharp increase in the coal concentration indicates the location of the pyrolysis front. Therefore, the rate of the pyrolysis front can be obtained from the coal concentration profile. For the current configuration, it was approximately 1 m/day.

5.2. Case 2: simulation of pyrolysis process

The pyrolysis process is a complex thermal decomposition of coal in the absence of oxygen in the temperature range of

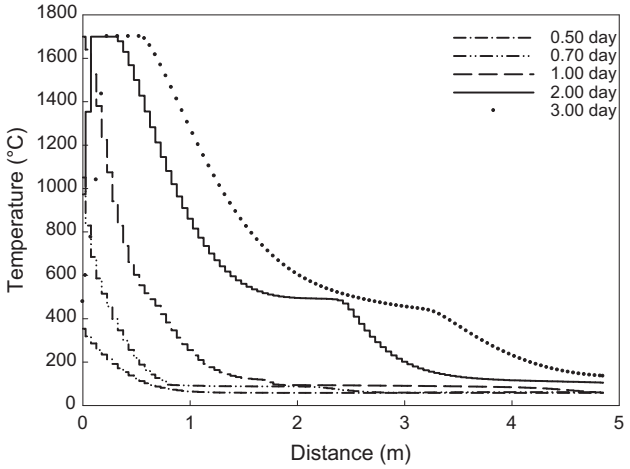

Fig. 5. Temperature profile at different times.

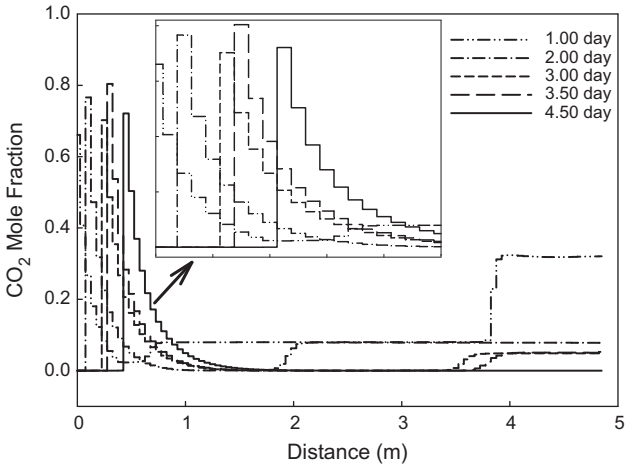

Fig. 6. Carbon dioxide profile at different times.

350–900 °C. During this process, coal is converted into low-molecular-weight gases, light hydrocarbons, and char. Each volatile matter is released from coal at different temperature ranges and rates. They also begin to evolve at different temperatures. Moreover, some species, such as CO_2 and CH_4, undergo several maximum rates of evolution, due to the cracking and carbonate decomposition reactions.

There are two widely applied methods to model pyrolysis. In the single-step decomposition method, the evolution of all species is modeled with only a single reaction. With the method of simultaneous-independent reactions for each species, it is assumed that the reactions are of the first order and Arrhenius type, the heating rate is constant, and the integral of the exponent term is approximated by Eq. (7). Therefore, the rate of evolution and cumulative amount of the ith volatile matter released by time t can be obtained analytically by Eqs. (8) and (9), respectively [13].

$$\int_0^T \exp\left(-\frac{E_{ai}}{RT}\right)dT = \left(\frac{RT^2}{E_{ai}}\right)\exp\left(-\frac{E_{ai}}{RT}\right) \tag{7}$$

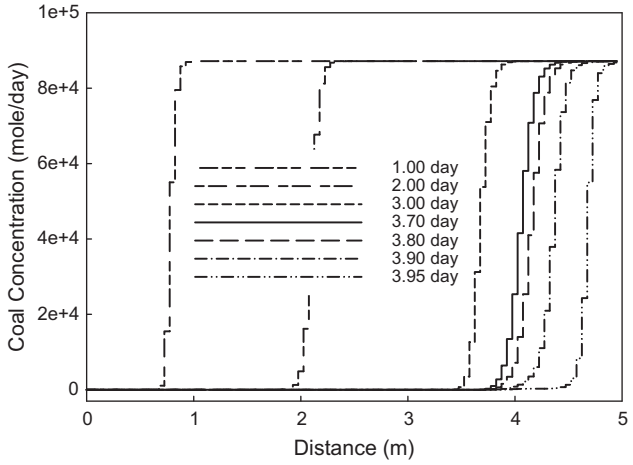

Fig. 7. Coal concentration profile at different times.

Table 3
Properties of components and pyrolysis reactions for Case 2.

Component	m_i^* gr i/gr coal	A_{0i} (1/s)	E_{ai} (kJ/mol)	MW_i (g/mol)
CO	0.034300	1766	111.11	28.01
CO_2	0.066830	403.1	88.43	44.01
CH_4	0.028700	7.322E+04	135.61	16.043
C_2H_6	0.005310	1.667E+06	139.84	30.07
C_3H_8	0.002784	7.333E+06	146.54	44.097
C_2H_4	0.001540	2.333E+06	139.84	28.054
H_2	0.006670	20	93.37	2.016
H_2O	0.112370	0.11469	31.09	18.015
Tar	0.037890	0.11469	31.09	600

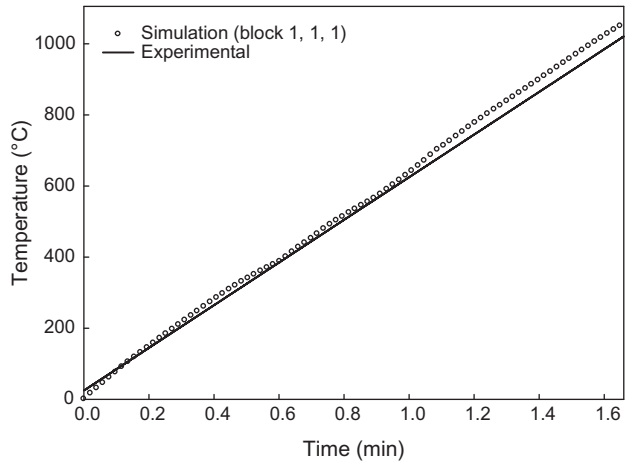

Fig. 8. Temperature comparison of the first block of the simulation model and the experimental test.

$$\frac{dm_i}{dT} = m_i^* \cdot \frac{A_{0i}R}{\beta E_{ai}}\exp\left(-\frac{E_{ai}}{RT}\right)\left(2T + \frac{E_{ai}}{R}\right) \cdot \exp\left(-\frac{A_{0i}RT^2}{\beta E_{ai}}\exp\left(-\frac{E_{ai}}{RT}\right)\right) \tag{8}$$

$$m_i = m_i^* \cdot \left[1 - \exp\left(-\frac{A_{0i}RT^2}{\beta E_{ai}}\exp\left(-\frac{E_{ai}}{RT}\right)\right)\right] \tag{9}$$

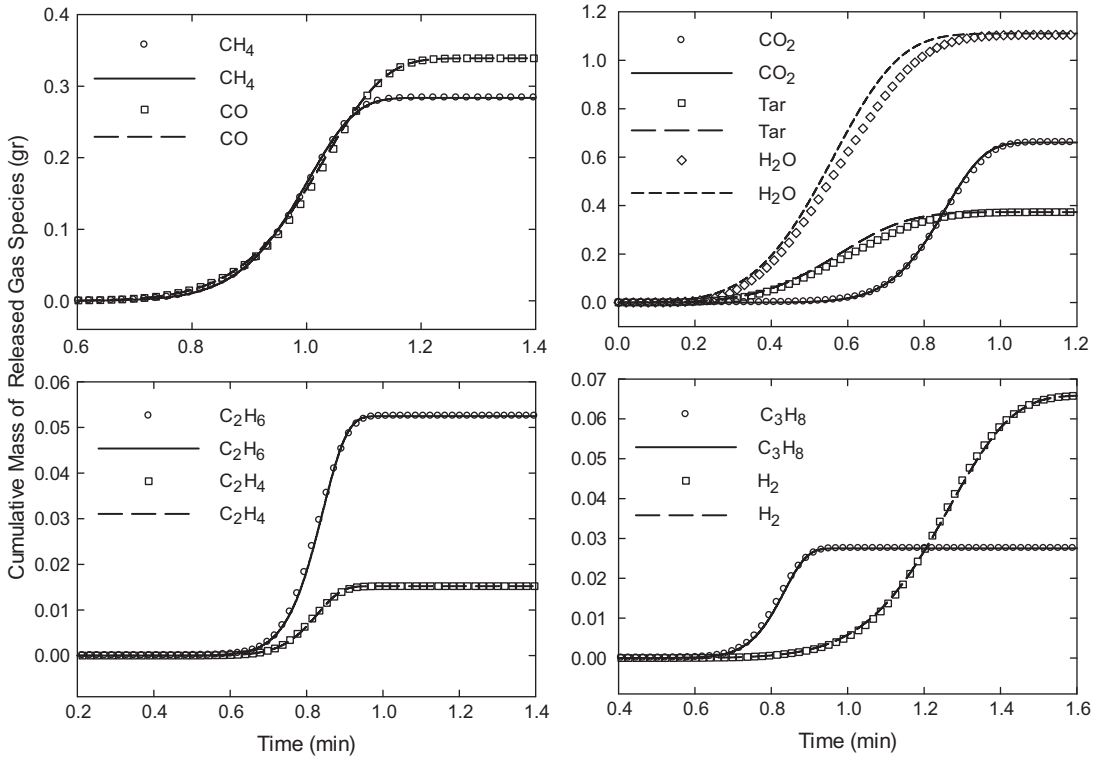

Fig. 9. Comparison of cumulative mass of produced gas species during pyrolysis process for analytical (lines) and simulation (symbols) results using simultaneous-independent reactions model.

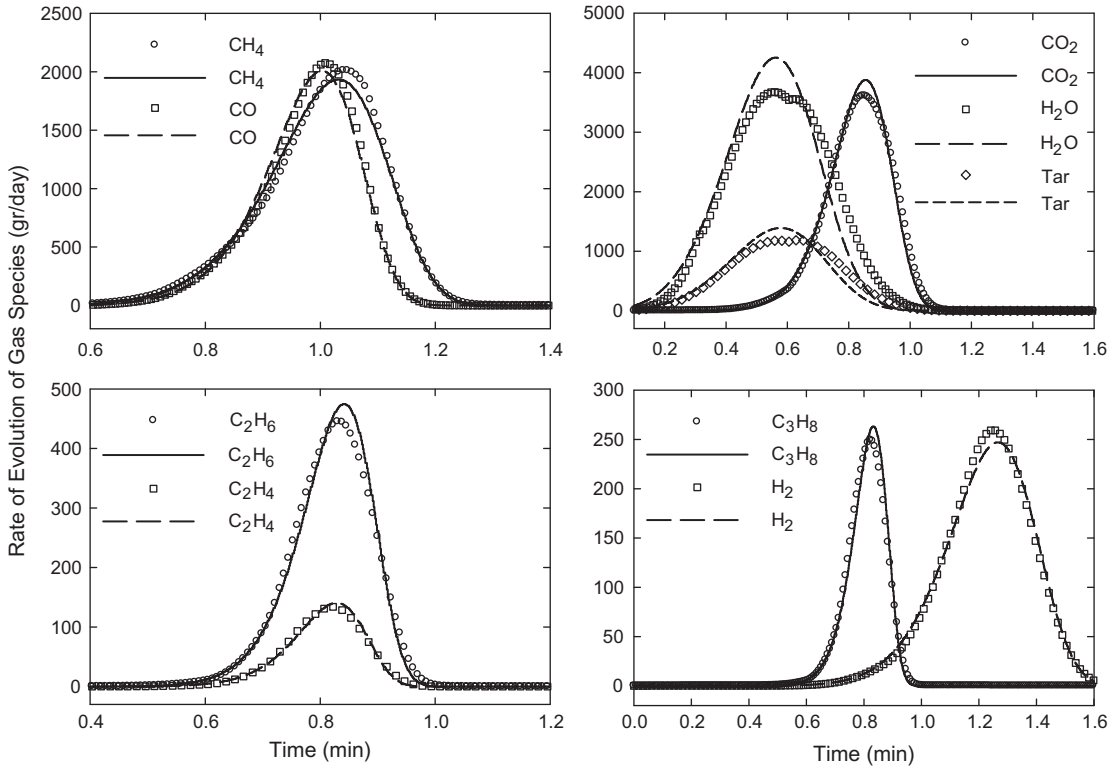

Fig. 10. Comparison of rate of evolution of gas species during pyrolysis process for analytical (lines) and simulation (symbols) results using simultaneous-independent reactions model.

In this section, the development of a simulation model for the modeling of the pyrolysis process using the two previously described methods and the matching of the results of the analytical method are presented. The simulation model included two blocks. The first block sized 5 * 1 * 1 cm contained coal and a heater. The second block did not have coal, due to the

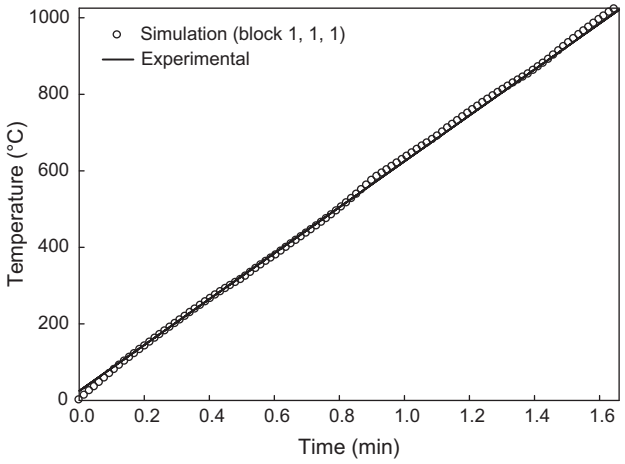

Fig. 11. Temperature comparison in the first block of the simulation model (single-step decomposition) and the experimental test.

temperature gradient effect. An injector was placed in the first block to inject nitrogen (N_2) as the carrier gas at a rate of 0.3 m^3/day, and a producer was placed in the second block. Nine gas components – H_2O, CO, H_2, CO_2, CH_4, ethane (C_2H_6), propane (C_3H_8), ethylene (C_2H_4), and tar – were assumed to evolve during the pyrolysis process. Therefore, there were nine reactions in the model. The heating rate of 10 °C/min was used for the analytical model. The properties of these components and relevant reactions are summarized in Table 3 [13].

In this model, the reaction material balance must be honored; hence, nine pseudo-solid species have been defined with the same molecular weight as each volatile matter, so that in each reaction this pseudo-solid species was converted into the corresponding volatile matter [14].

Fig. 8 illustrates the variation of temperature in the first block of the simulation model and the experimental test. In this experiment, the heating rate and initial temperature were assumed to be 10 °C/min and 25 °C, respectively. The temperature was matched by changing the rate of heat injection, i.e., the heater rate. In the late part of the experiment, the solid content in the domain decreased, and the convection heat transfer played a dominant role; therefore, there was a poor temperature match.

The rate of evolution and cumulative released amount of each species are shown in Figs. 9 and 10. As can be seen, there was a good match between the simulation (dots) and analytical (solid lines) results. Moreover, this simulation model was able to precisely capture the onset of the evolution, the temperature range, and the maximum rate of evolution.

In the next step, pyrolysis was simulated using the single-step decomposition model for the same data set as listed in Table 3. The pyrolysis reaction was obtained using the elemental balance, coal analysis results, and the ultimate recovery of gaseous species during pyrolysis process from Tables II-2 and II-3 of Ref. [13]:

$$\begin{aligned} coal(daf) \rightarrow\ & 0.583598C + 0.029229CO + 0.036245CO_2 \\ & + 0.042700CH_4 + 0.004215C_2H_6 + 0.001507C_3H_8 \\ & + 0.001310C_2H_4 + 0.078971H_2 + 0.148884H_2O \\ & + 0.001502Tar \end{aligned}$$

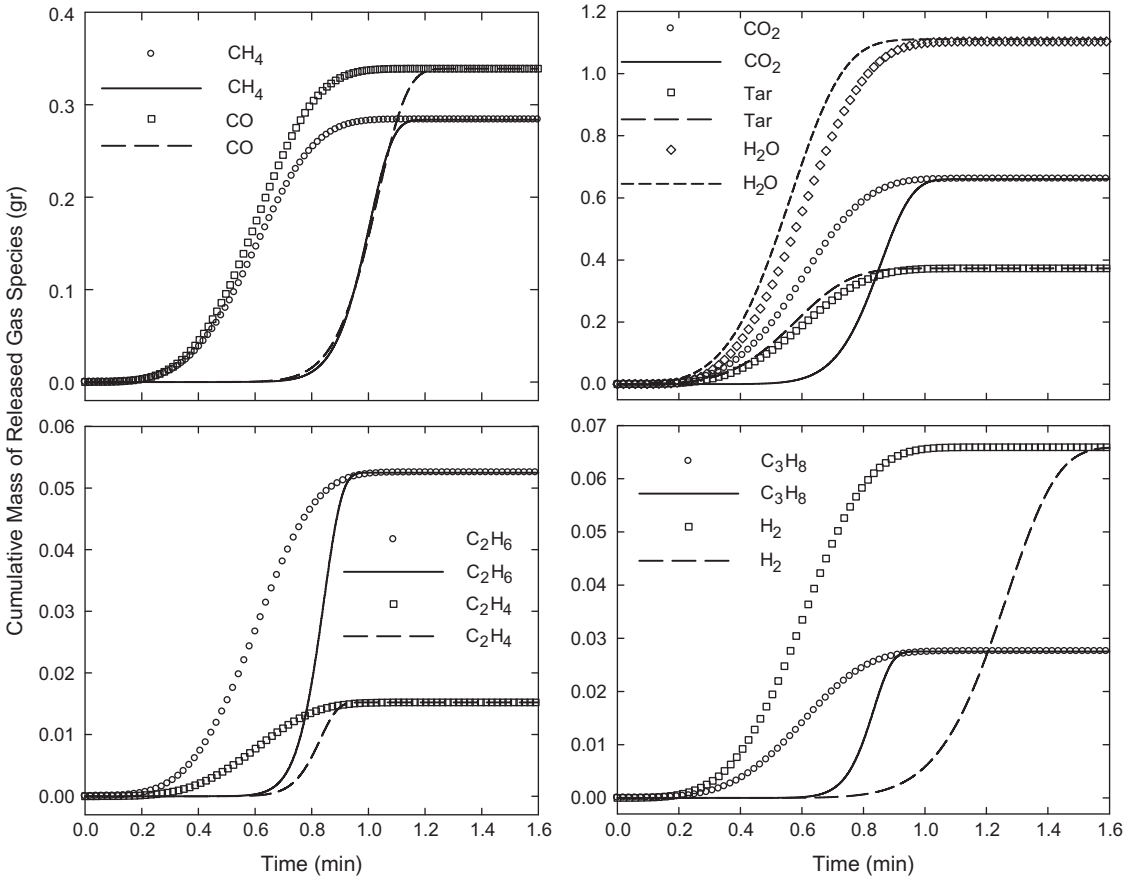

Fig. 12. Comparison of cumulative produced gas species during pyrolysis process for analytical (lines) and simulation (symbols) results applying single-step decomposition model.

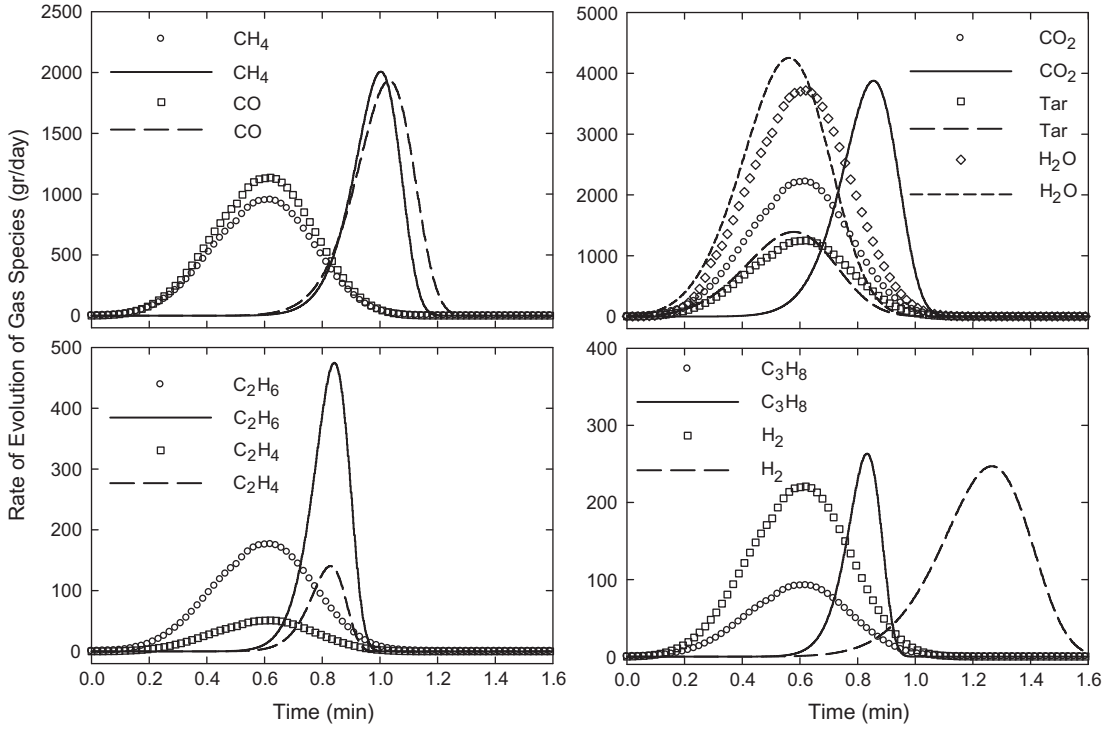

Fig. 13. Comparison of rate of produced gas species during pyrolysis process for analytical (lines) and simulation (symbols) results applying single-step decomposition model.

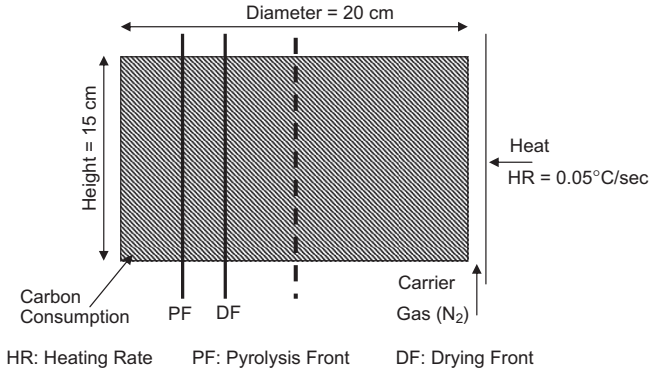

Fig. 14. Schematic of the experiment of coal self-gasification.

Fig. 11 shows a very good match for temperature. However, as can be seen in Figs. 12 and 13, the cumulative amount of the species and the rate of evolution did not match with the analytical model. Moreover, all species began to evolve at the same temperature and range of temperatures. This is due to the use of only single activation energy for the evolution of all volatile matters during the complex pyrolysis process.

5.3. Case 3: simulation of self-gasification experiment

In this section, a description of the simulation of the self-gasification experiment is provided. As shown in Fig. 14, the external surface of a vertical cylindrical coal core with a diameter of 20 cm and a height of 15 cm was heated at a heating rate of 0.05 °C/s at the atmospheric pressure. As a result of the heat conduction, the moisture content of the coal evaporated, and pyrolysis took place within the coal. Thus, the heat flowed from the outer surface into the center of the coal; and, there was a mass flux towards outside of the coal. Therefore, both the drying and pyrolysis fronts advanced towards the center of the core. N_2 was used as the carrier gas to sweep away the volatile matter. In this experiment, the temperature was recorded at different locations and times [13,15].

To simulate this experiment, a cylindrical model with the same dimensions was developed in Computer Modelling Group Inc.'s STARS simulation software. The producer and injector were placed in the most outer block. A heater was used in this block to provide the heat requirement. Pyrolysis was modeled by the simultaneous-independent reactions method. Steam gasification, Boudouard, methanation, and water–gas-shift reactions were applied in this model, according to Table 2. The temperature was matched by changing the heat injection rate of the heater.

Fig. 15 illustrates the temperature profiles from the center of core to its surface at different times based on surface temperature. As can be seen, there was a good agreement between the simulation and experimental results. Since this experiment was conducted at the atmospheric pressure, the saturation temperature of water was about 100 °C. Thus, the deviation of the temperature from 100 °C is an indication of the location of the vaporization front, which moves towards the center of the core.

Temperature increased from the drying front towards the surface where the heater was located. In this region, the pyrolysis process took place. Since pyrolysis was modeled using the simultaneous-independent reactions method, each species has its own evolution onset temperature. Therefore, the pyrolysis front can be investigated according to the evolution of each species, as shown in Fig. 16. The tar front at time 3.5 h was faster than that of the other species, which indicates that the activation energy for tar was less than the others and caused the early evolution of tar, although its frequency factor was significantly smaller. On the other hand, the hydrogen front was the slowest one, due to its larger activation energy and small frequency factor for hydrogen evolution, which implies that hydrogen evolved at a higher

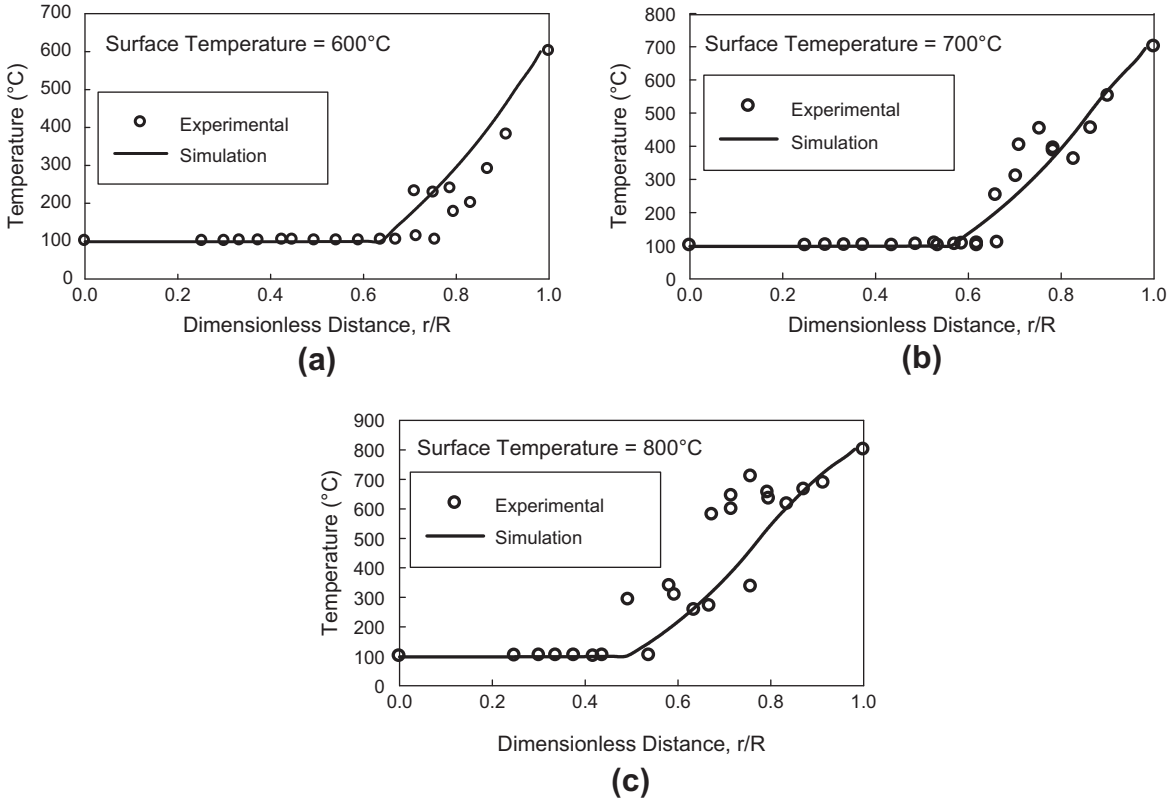

Fig. 15. Temperature profile at times when the surface temperature was: (a) 600 °C, (b) 700 °C, and (c) 800 °C.

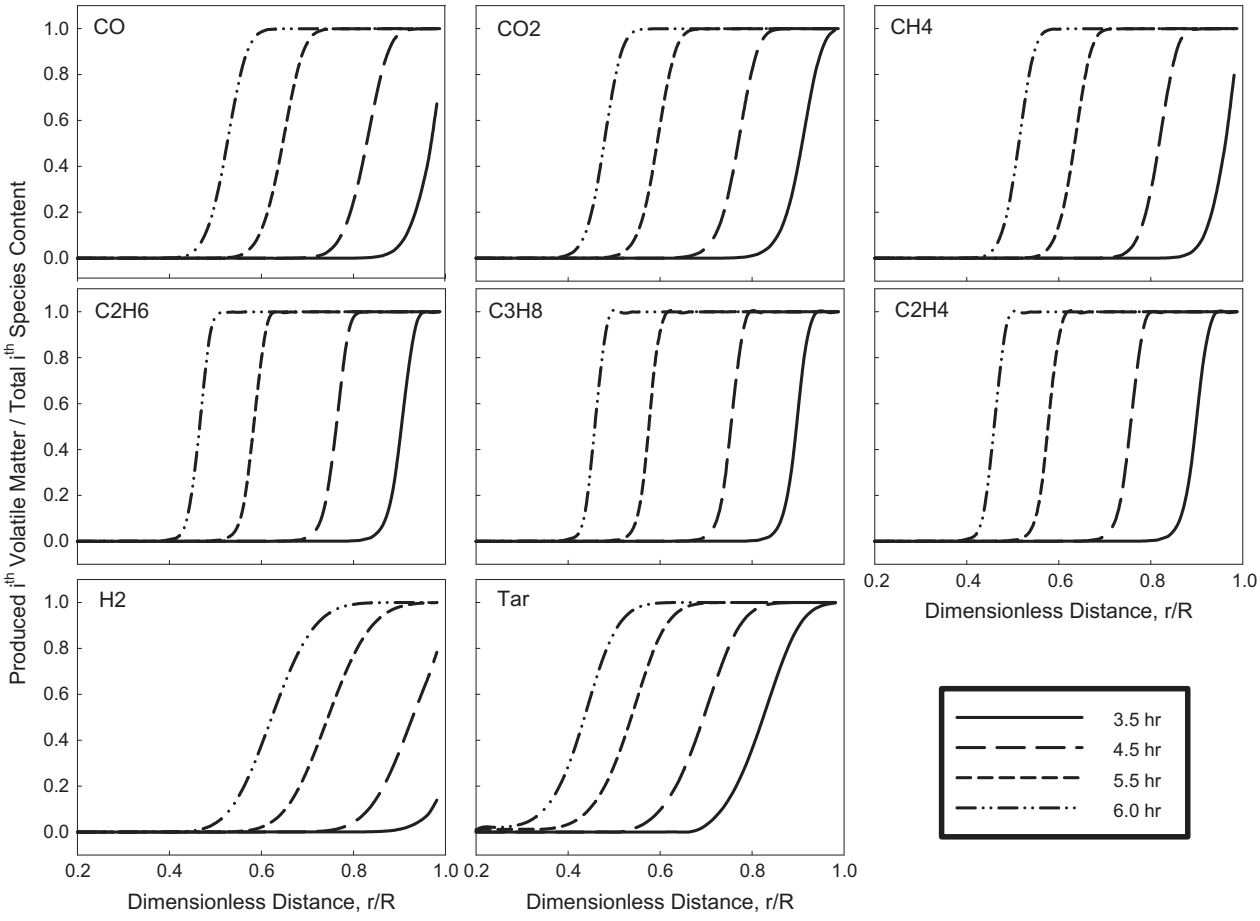

Fig. 16. Profile of the fraction of the cumulative evolved species from coal.

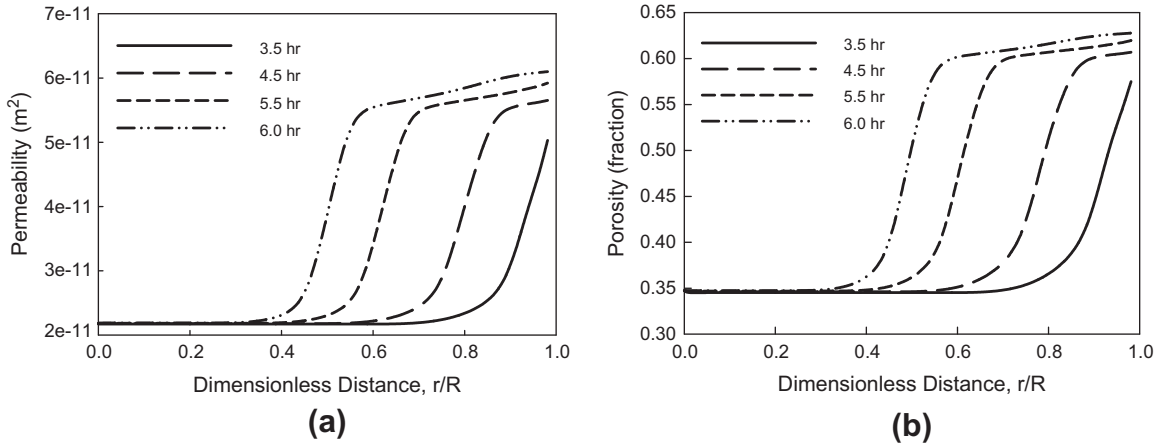

Fig. 17. Profiles of (a) permeability and (b) porosity at different times.

temperature. The pyrolysis front for light hydrocarbon gases and carbon oxides were almost at the same order of magnitude; hence, these species began to evolve at approximately the same temperature.

Fig. 17 shows the variation of permeability and porosity with temperature from the center of core towards its surface at different times. As can be seen, the porosity and permeability increased from the location of the drying front towards the surface of the core. The sharp changes in these parameters were an indication of partial and complete pyrolysis regions, as this was where they obtained their highest values. However, due to the existence of char and hot volatile matter, heterogeneous reactions, such as steam gasification and Boudouard reactions, become active close to the surface of the core. This process is called self-gasification, in which char is gasified by the species released during the pyrolysis and vaporization processes. Self-gasification causes an increase in the porosity and permeability of the core near its surface where solid materials, such as carbon, are consumed. Therefore, the highest porosity and permeability during self-gasification is on the surface of the core.

6. Conclusions

This paper proposed a procedure to obtain the physical properties of the solid materials required by porous medium simulators from the basic elemental and proximate analyses of coal. This procedure and relevant assumptions and proposed workflow to build the structure of the domain were evaluated through the simulation of three processes, i.e., the combustion tube test, pyrolysis, and self-gasification. The acceptable agreement of the results of the simulation, the analytical method and the experiment emphasized the reliability of the proposed procedure and assumptions. Moreover, it can be concluded that the developed numerical simulation model for the pyrolysis process can be used to match the experimental data to obtain the kinetics of the evolution of each species. This is important for cases where cracking and carbonate decomposition phenomena are significant, because the analytical model does not consider these reactions. In addition, in spite of the greater accuracy of the simultaneous-independent reactions method compared to the single-step decomposition method for modeling of the pyrolysis process, the former method can be very expensive in large-scale simulations of the UCG process using the porous medium approach, due to the requirement of a large number of components and reactions in the simulation model.

Acknowledgements

This study was supported by the Department of Chemical and Petroleum Engineering at the University of Calgary, Natural Sciences and Engineering Research Council of Canada, Alberta Innovates, and Foundation CMG.

Appendix A. Supplementary material

Supplementary data associated with this article can be found, in the online version, at http://dx.doi.org/10.1016/j.fuel.2013.07.091.

References

[1] Shirsat Arvind V. Modeling of cavity growth in underground coal gasification. MSc. thesis. Texas Tech University; May 1989.
[2] Yonggang Luo, Coertzen M, Dumble S. Comparison of UCG cavity growth with CFD model predictions. In: Seventh international conference on CFD in the minerals and process industries. Australia: Melbourne: CSIRO; December 2009. p. 9–11.
[3] Perkins G. Mathematical modeling of underground coal gasification. PhD dissertation. The University of New South Wales; 2005.
[4] Massaquoi JGM. Combustion in underground coal conversion. PhD dissertation. West Virginia University; 1981.
[5] Britten JA, Thorsness CB. A mechanistic model for axisymmetric cavity growth during underground coal gasification. American Chemical Society; 1988.
[6] Magnani CF. Mathematical foundations for the process of underground coal. PhD dissertation. The Pennsylvania State University; 1973.
[7] Winslow AM. Numerical model of coal gasification in a packed bed. Symposium (International) on combustion; January 1977. vol. 16. p. 503–513.
[8] Batenburg van DW. Heat and mass transfer during underground gasification of thin deep coal seams. PhD dissertation. Delft University of Technology; 1992.
[9] Biezen ENJ. Modeling underground coal gasification. PhD dissertation. Delft University of Technology; 1996.
[10] Yang L. Numerical study on the underground coal gasification for inclined seams. AIChE J. 2005;51(11).
[11] Seifi M, Chen Z, Abedi J. Numerical simulation study of underground coal gasification using the CRIP method. Canad J Chem Eng 2011;89:6.
[12] Green DW, Willhite GP. Enhanced oil recovery. Richardson, Tex., Society of Petroleum Engineers; 1998.
[13] Tsang THT. Modeling of heat and mass transfer during coal block gasification. PhD dissertation. The University of Texas at Austin; 1980.
[14] Computer Modeling Group. STARS Technical Manual.
[15] Forrester III RC, Westmoreland PR. Two-dimensional pyrolysis effects during in situ coal gasification: preliminary results. J. Pet. Tech. 1979:571.